Acta Cryst. (1990). B46, 620–628

Disordered Incommensurate Structure of $[N(CH_3)_4]_2CuBr_4$ at 248 K

BY G. MADARIAGA, F. J. ZÚÑIGA AND W. A. PACIOREK†

Departamento de Física de la Materia Condensada, Facultad de Ciencias, Universidad del País Vasco, Apdo 644, *Bilbao, Spain*

AND E. H. BOCANEGRA

Departamento de Física Aplicada II, *Facultad de Ciencias, Universidad del País Vasco, Apdo* 644, *Bilbao, Spain*

(*Received* 12 *March* 1990; *accepted* 15 *May* 1990)

Abstract

The structure of the incommensurate phase of bis(tetramethylammonium) tetrabromocuprate(II), $[N(CH_3)_4]_2CuBr_4$, has been determined at 248 K in the superspace group $P(Pmcn):(s\bar{1}1)$. Intensities including main and first-order satellites were used in the refinement of several models. The best results were obtained using both displacive and occupational probability modulations in the harmonic approximation. Convergence of the refinement process was only possible by means of soft restrictions for the interatomic distances. The corresponding final agreement factors are $R = 0{\cdot}054$, $R_0 = 0{\cdot}046$ and $R_1 = 0{\cdot}092$ for all, main and satellite reflections respectively. This model suggests the presence of an important degree of disorder in the incommensurate phase. The reliability of the model has been confirmed by comparison between the extrapolated commensurate distortion and the lock-in structure. A comparison with the structure of $[P(CH_3)_4]_2CuBr_4$ at 293 K is also reported. Crystal data of the average structure: $M_r = 531{\cdot}45$, orthorhombic, *Pmcn*, $a = 9{\cdot}331$ (1), $b = 15{\cdot}708$ (2), $c = 12{\cdot}598$ (3) Å, $V = 1846{\cdot}5$ (9) Å^3, $Z = 4$, $D_x = 1{\cdot}91$ Mg m^{-3}, λ(Mo $K\alpha$) $= 0{\cdot}7107$ Å, $\mu = 10{\cdot}31$ mm^{-1}, $F(000) = 1020$, wavevector $\mathbf{q} = 0{\cdot}604\ (3)\mathbf{b}^*$.

Introduction

$[N(CH_3)_4]_2CuBr_4$ is unique compared with the bis(tetramethylammonium) tetrabromometallates $\{[N(CH_3)_4]_2MBr_4$, M = Zn, Co and Mn$\}$ reported to date (Gesi, 1982, 1983; Hasebe, Mashiyama & Tanisaki, 1985; Asahi, Hasebe & Gesi, 1988), mainly owing to the presence in its phase-transition scheme of an incommensurate (IC) phase, followed by a ferroelectric commensurate (lock-in) phase. The transition temperatures (on cooling) together with the space groups for the normal (N) and the lock-in (F) structures and the modulation wavevectors of the incommensurate and lock-in phases (López-Echarri, Ruiz-Larrea & Tello, 1989; Trouelan, Lefebvre & Derollez, 1984; Hasebe, Mashiyama & Tanisaki, 1985) are indicated below.

$$\underset{Pmcn}{N} \xrightarrow{270{\cdot}7\ (1)\ K} \underset{\mathbf{q}=\alpha\mathbf{b}^*}{IC} \xrightarrow{241{\cdot}7\ (1)\ K} \underset{Pbc2_1\ (\mathbf{q}=0{\cdot}5\mathbf{b}^*)}{F}$$

The most important difference between this compound and the majority of tetramethylammonium tetrahalogenometallate crystals studied up to now is that the modulation direction is along **b*** rather than **c*** (in the same setting of reciprocal axes).

The structure of the normal phase shows unusually large values for the thermal parameters. This fact suggests the presence of orientational disorder (Trouelan, Lefebvre & Derollez, 1984). Consequently, Hasebe, Mashiyama & Tanisaki (1985) have proposed a structural model in which the atoms are split with respect to the $\{\sigma_x|\frac{1}{2}00\}$ plane. Although this model does not produce any improvement in the R-factor value, it can be justified within the analysis of the atomic mean-square amplitudes of thermal vibration, performed at several temperatures for the inorganic tetrahedron.

On the other hand, the twofold (along **b**) lock-in structure (Hasebe, Mashiyama & Tanisaki, 1985) seems to be perfectly ordered. As a second structural characteristic, common to both structures, it is worth noting the presence of an important Jahn–Teller distortion of the $[CuBr_4]^{2-}$ ions (Trouelan, Lefebvre & Derollez, 1984; Hasebe, Mashiyama & Tanisaki, 1985), which is also present in $[N(CH_3)_4]_2CuCl_4$ (Clay, Murray-Rust & Murray-Rust, 1975).

The presence of orientational disorder has also been pointed out as a result of specific heat measurements (López-Echarri, Ruiz-Larrea & Tello, 1989). The analysis of thermodynamic functions shows that

† On leave of absence from the Institute for Low Temperature and Structure Research, Polish Academy of Sciences, pl. Katedralny, 50–950 Wrocław, Poland.

0108-7681/90/050620-09$03.00

complete ordering should take place in the phase transition, which relates the lock-in phase to the next monoclinic ferroelastic structure at lower temperature. This suggests the existence of a decreasing, but important, amount of disorder in the incommensurate structure.

If these arguments are taken into account, it is then necessary from a structural point of view to allow for modulation of the atomic occupational probability together with the more usual positional descriptors of incommensurate structures. Such a mixed model has never been used in incommensurate structure determinations of A_2BX_4 compounds although the order–disorder character of the normal–incommensurate phase transition has been claimed for several members of this family.

In this work we present a model for the incommensurate structure of $[N(CH_3)_4]_2CuBr_4$ which includes mixed (positional and occupational) modulation. Its reliability is checked by comparison of the commensurate distortion of the lock-in phase for this compound and for the isomorphous $[P(CH_3)_4]_2CuBr_4$ at room temperature (Madariaga, Alberdi & Zúñiga, 1990) with the corresponding extrapolated distortion from the refined incommensurate structure.

Experimental

Dark-violet single crystals of $[N(CH_3)_4]_2CuBr_4$ suitable for X-ray measurements were obtained by slow evaporation at 298 K of an aqueous solution of $N(CH_3)_2Br$ and $CuCl_4$ in stoichiometric proportions.

A set of precession photographs were taken at several temperatures within the incommensurate phase, in order to determine the best conditions for data collection. Temperature control was performed using an open N_2-flow cryostat (Cosier & Glazer, 1986). Temperature stability was ±0·2 K during the complete experiment. The photographs showed orthorhombic symmetry, and a significant number of first-order satellites could be identified. The systematic absences detected for the main reflections were compatible with space group *Pmcn*. A careful investigation of the $(h,k,0,1)$ reflections allowed the determination of the approximate (in the sense that no higher-order satellites were observed) extinction rules:

$$hk0m \quad h+k=\text{odd} \quad (m>0)$$
$$0k0m \quad m=\text{odd} \quad (k=\text{odd})$$

the second rule being a special case of the more general systematic absence:

$$0klm \quad m=\text{odd}$$

which indicates the existence of a $\{\sigma_x|\frac{1}{2},0,0,\frac{1}{2}\}$ mirror plane in the superspace group. At this point, given the observed wavevector ($\mathbf{q} \approx 0{\cdot}6\mathbf{b}^*$), the superspace group $P(Pmcn):(s\bar{1}1)$ (de Wolff, Janssen & Janner, 1981) was assumed.

Table 1. *Summary of crystal data and data-collection parameters*

Crystal form	Polyhedral
Crystal size (mm)	0·12 × 0·19 × 0·18
Temperature	248·0 (2) K
Reflections for lattice-parameters refinement	19 ($9{\cdot}5 < \theta < 27°$)
Cell parameters (Å)	a = 9·331 (1)
	b = 15·708 (2)
	c = 12·598 (3)
$(\sin\theta/\lambda)_{max}$ (Å^{-1}) ($hkl0$)	0·704
$(\sin\theta/\lambda)_{max}$ (Å^{-1}) ($hklm$)	0·364
Check reflections	3 main reflections
$h,k,l,0$ limits	(0–13 ±22 ±17)
h,k,l,m limits	(±6 0–10 0–9 ±1)
Scan width (°)	$0{\cdot}65 + 0{\cdot}34\tan\theta$
Scan speed (° min^{-1})	0·72–8·25
Measured reflections	
Total	13199
Main	11452
First satellite	1747
Independent reflections	
Main (observed $I > 3\sigma$)	2827 (571)
Satellite (observed $I > 3\sigma$)	654 (270)
R_{int} without absorption correction	0·147
R_{int} with absorption correction	0·111
Transmission (max./min.)	0·3510/0·1814
Weights	Unit weights and $1/\sigma^2(F)$
Max. shift/e.s.d.	0·67

Crystal data and data-collection parameters are summarized in Table 1. A more accurate wavevector value, $\mathbf{q} = 0{\cdot}604\ (3)\mathbf{b}^*$, was obtained from the profile of scanned satellite reflections along $\mathbf{b}^*$. Intensities were collected in the following sequence: first, main reflections and then satellites in the order $(h,k,l,\pm m)$. Gaussian absorption correction and internal scaling were carried out using a local version of the program system *XRAY*72 (Stewart, Kruger, Ammon, Dickinson & Hall, 1972) modified for one-dimensionally modulated structures. Lorentz and polarization corrections were performed during refinement with the program *MSR* (Paciorek & Kucharczyk, 1985; Paciorek & Uszynski, 1987) and will be described in a subsequent section.

Symmetry and description of the incommensurate phase

As already indicated, the superspace group of the incommensurate phase of $[N(CH_3)_4]_2CuBr_4$ is $P(Pmcn):(s\bar{1}1)$. The elements of this group (obviating superspace translations) are given in Table 2. The operations are indicated in the form $\{\mathbf{R}|\mathbf{t},\tau\}$, where $\mathbf{R}$ is the rotational operation, $\mathbf{t}$ the fractional translation and τ the shift along the internal space (Yamamoto, 1982; Pérez-Mato, Madariaga, Zúñiga & García-Arribas, 1987). As can be seen in the table, the internal translation τ depends in general on the value of the modulation wavevector and on the

Table 2. *Representative elements of the superspace group P(Pmcn):($s\bar{1}1$) with* $\mathbf{q} = \alpha\mathbf{b}^*$

$\{E\|0,0,0,0\}$	$\{I\|0,0,0,\Phi/\pi\}$
$\{C_{2x}\|\frac{1}{2},0,0,\Phi/\pi+\frac{1}{2}\}$	$\{\sigma_x\|\frac{1}{2},0,0,\frac{1}{2}\}$
$\{C_{2y}\|0,\frac{1}{2},\frac{1}{2},-\alpha/2+\frac{1}{2}\}$	$\{\sigma_y\|0,\frac{1}{2},\frac{1}{2},-\alpha/2+\Phi/\pi+\frac{1}{2}\}$
$\{C_{2z}\|\frac{1}{2},\frac{1}{2},z,-\alpha/2+\Phi/\pi\}$	$\{\sigma_z\|\frac{1}{2},\frac{1}{2},z,-\alpha/2\}$

Generators of the superlattice

$\{E|1,0,0,0\}$ $\{E|0,1,0,-\alpha\}$ $\{E|0,0,1,0\}$ $\{E|0,0,0,1\}$

arbitrary choice of origin along the internal space which is fixed by the value assigned to the global phase Φ in Table 2 (in this work Φ was set to zero).

The extinction rules resulting from the elements of this superspace group can be easily deduced (Janner & Janssen, 1980) and summarized as follows:

$$0klm \qquad m = \text{odd}$$
$$h0l0 \qquad l = \text{odd}$$
$$hk0m \qquad h+k = \text{odd}.$$

These extinction rules include as subcases those resulting from the other operations and are caused by the symmetry operations $\{\sigma_x|\frac{1}{2},0,0\frac{1}{2}\}$, $\{\sigma_y|0,\frac{1}{2},\frac{1}{2},-\alpha/2+\frac{1}{2}\}$ and $\{\sigma_z|\frac{1}{2},\frac{1}{2},\frac{1}{2},-\alpha/2\}$ respectively. As can be seen these systematic absences were found in the precession photographs. The collected reflections also satisfy these extinction conditions.

The modulated structure of $[N(CH_3)_4]_2CuBr_4$ will be described, in its most general form, by two different modulated parameters. On the one hand the atomic position of atom μ in cell $\mathbf{l}$ can be written in the form:

$$\mathbf{r}(\mathbf{l},\mu) = \mathbf{l} + \mathbf{r}^{\mu}_{\text{av}} + \tfrac{1}{2}\sum_n \mathbf{u}^{\mu}_n \exp[2\pi n\mathbf{q}.(\mathbf{l}+\mathbf{r}^{\mu}_{\text{av}})] \quad (1)$$

where $\mathbf{r}^{\mu}_{\text{av}}$ is the position of the atom in the average structure and the amplitudes $\mathbf{u}^{\mu}_n$ satisfy $\mathbf{u}^{\mu}_n = \mathbf{u}^{\mu^*}_{-n}$.

On the other hand when a disordered (or mixed) model is assumed, it is also necessary to consider the modulation of the atomic occupation probability in the form:

$$P(\mathbf{l},\mu) = P^{\mu}_{\text{av}} + \tfrac{1}{2}\sum_n P^{\mu}_n \exp[2\pi n\mathbf{q}.(\mathbf{l}+\mathbf{r}^{\mu}_{\text{av}})], \quad (2)$$

P^{μ}_{av} being the occupational probability for atom μ in the average structure and $P^{\mu}_n = P^{\mu^*}_{-n}$.

If two atoms μ, ν are related in the average structure by the symmetry operation $\{\mathbf{R}|\mathbf{t}\}$ ($\{\mathbf{R}|\mathbf{t},\tau\}$ being an operation of the superspace group) the Fourier vectorial amplitudes $\mathbf{u}^{\mu}_n$, $\mathbf{u}^{\nu}_n$ and the scalar ones P^{μ}_n, P^{ν}_n are related by (Pérez-Mato, Madariaga, Zúñiga & García-Arribas, 1987):

$$\mathbf{u}^{\nu}_n = \mathbf{R}\,\mathbf{u}^{\mu}_{\Gamma(R)n}\exp(-i2\pi n\tau_0) \quad (3)$$

$$P^{\nu}_n = P^{\mu}_{\Gamma(R)n}\exp(-i2\pi n\tau_0) \quad (4)$$

where $\Gamma(R) = \pm 1$ if $\mathbf{Rq} = \pm\mathbf{q}$ and $\tau_0 = \tau + \mathbf{q}.\mathbf{t}$.

In the superspace group $P(Pmcn)$:($s\bar{1}1$) there are symmetry restrictions on the atomic parameters of atoms lying on the phase glide plane $\{\sigma_x|\frac{1}{2},0,0,\frac{1}{2}\}$. In this type of compound, such special positions are normally occupied by the central and two peripheral atoms of both the inorganic and the organic tetrahedra. As will be shown, one of the refined models corresponds to this atomic configuration. In this case expression (3) is rewritten in the form:

$$u^{\mu}_{n,x} = (-1)^{n+1}u^{\mu}_{n,x}$$
$$u^{\mu}_{n,(y,z)} = (-1)^{n}u^{\mu}_{n,(y,z)}$$

which implies that

$$u^{\mu}_{n,x} = 0 \qquad n = \text{even}$$
$$u^{\mu}_{n,(y,z)} = 0 \qquad n = \text{odd}.$$

Obviously for this model $P^{\mu}_{av} = 1$ and $P^{\mu}_n = 0$ for every n.

Structure refinement

The average structure was previously refined with the *XRAY*72 system using only the main reflections. Starting from the atomic positions at room temperature published by Trouelan, Lefebvre & Derollez (1984) the refinement process was continuously divergent after several isotropic cycles. The model obtained showed an atomic disposition in which almost all the interatomic distances were physically unreasonable. In general, this behaviour is associated with an insufficient number of observations per refined parameter. This problem was solved when soft restrictions for the Cu—Br and N—C interatomic distances together with the structure factors were used as 'observed' quantities. After several anisotropic cycles the refinement converged to an R value of 0·065.

The analysis of the atomic thermal ellipsoids suggested the presence of orientational disorder. Therefore all atoms were split into two symmetric positions with respect to the σ_x mirror plane. After anisotropic refinement of this model the R factor reached a value of 0·043. In the last cycles an anisotropic extinction correction was included. Any attempt to reduce the number of positional parameters (partially splitting the structure) failed.

Refinement of the incommensurate structure was carried out with the program *MSR* (Paciorek & Kucharczyk, 1985; Paciorek & Uszynski, 1987) using, as variables for the atomic modulation functions, the moduli and phases of the Fourier amplitudes (Zúñiga, Madariaga, Paciorek, Pérez-Mato, Ezpeleta & Etxebarria, 1989) in the expansion:

$$u^{\mu}_{\alpha}(t) = \sum_{n>0} A^{\mu}_{n,\alpha}\cos[2\pi(nt+\varphi^{\mu}_{n,\alpha})] \quad (\alpha = x, y, z) \quad (5)$$

$$P^{\mu}(t) = \sum_{n>0} P^{\mu}_n \cos[2\pi(nt+\psi^{\mu}_n)] \quad (6)$$

where t is the internal coordinate, ranging from 0 to 1, which corresponds to the dense set of fractional values $\mathbf{q}.(\mathbf{l}+\mathbf{r}^{\mu}_{av})$ in (1) and (2). The parametrization was chosen because of its flexibility when linear relationships between phases are required. The infinite series (5) and (6) were restricted to the first harmonic as only first-order satellites were observed.

Refinements were based on $|F|$ and performed in the full-matrix mode, initially with unit weights. In every cycle a common scale factor for main and satellite reflections as well as an isotropic extinction correction, described in Zúñiga, Madariaga, Paciorek, Pérez-Mato, Ezpeleta & Etxebarria (1989) were refined. The scattering factors for neutral atoms and the anomalous-dispersion correction were taken from *International Tables for X-ray Crystallography* (1974). Plots of the structures were prepared using the programs *STRUPLO* (Fischer, 1985) and *SCHAKAL*88 (Keller, 1989). Two reflections (11,1,4,0 and 1,3,4,1), with intensities above but close to the observability threshold, were marked as unobserved during all refinement processes.

Four models of increasing complexity were tried. In model I, average positions of Cu and N atoms together with two Br and two C atoms were fixed in the $\{\sigma_x|\frac{1}{2}00\frac{1}{2}\}$ plane. The refined parameters in the last cycles were the remaining average coordinates, the moduli and phases of the first harmonic in (5), and the anisotropic thermal parameters for the Cu and Br atoms. The interatomic distances calculated as a function of the internal coordinate t showed quite reasonable values for the Cu—Br and N—C bonds. However, considerable distortion of the organic tetrahedra was evident from analysis of the C—C distances. It was clearly a Jahn–Teller distortion in the $[CuBr_4]^{2-}$ ion, also observed in both the normal and lock-in phases (Trouelan, Lefebvre & Derollez, 1984; Hasebe, Mashiyama & Tanisaki, 1985). The use of anisotropic thermal parameters for all the atoms (model II) did not introduce any important change in the R factors.

Nevertheless, the thermal parameters again indicated the possibility of disorder in the incommensurate phase. Therefore, after the first refinement of the average structure, the atoms were split with respect to the σ_x plane with a restricted homogeneous occupation probability equal to 0·5 (model III). Anisotropic thermal parameters were allowed only for the inorganic tetrahedron, in order to keep a reasonable ratio between the number of observations and the number of refined parameters. However, to achieve convergence of this refinement, implementation of soft restrictions for interatomic distances (Paciorek, Madariaga & Zúñiga, 1990) and constraint of all the possible Cu—Br, Br—Br, N—C and C—C distances were required. The decrease in the atomic thermal parameters (by more than 30% for some atoms) seems to confirm the presence of orientational disorder.

Table 3. *R factors and goodness of fit (S) for the analyzed models*

R (wR), R_0 (wR_0), R_1 (wR_1) are the R factors (weighted R factors) for all, main and satellite reflections, respectively. N is the number of refined parameters. PF refers to the use of a penalty function for interatomic distances in the corresponding model. wR/wR^{IV} is the weighted R ratio used in the Hamilton test (see text).

Model	PF	N	R wR	R_0 wR_0	R_1 wR_1	wR/wR^{IV}	S
I	No	91	0·076 0·089	0·065 0·081	0·135 0·148	1·4355	6·00
II	No	119	0·072 0·083	0·061 0·075	0·128 0·141	1·3387	5·73
III	Yes	177	0·056 0·064	0·048 0·058	0·097 0·107	1·0323	4·51
IV	Yes	183	0·054 0·062	0·046 0·057	0·092 0·100	1·0000	4·38

On the other hand in an incommensurate phase there is no reason to restrict the atomic occupational probability to the zeroth-order harmonic. For this reason the modulus and phase of the first harmonic component of expansion (6) were included in the refinement (model IV). From physical considerations only one complex amplitude per tetrahedron was considered. Thus, expression (6) was rewritten as follows:

$$P^{\mu}(t) = P^{\text{c.a.}}\cos[2\pi(t+\psi^{\mu})]$$

with

$$\psi^{\mu} = \psi^{\text{c.a.}} + \mathbf{q}.(\mathbf{r}^{\text{c.a.}}_{av} - \mathbf{r}^{\mu}_{av})$$

where the index c.a. refers to the parameters of the central atom of the tetrahedron to which the atom μ belongs. In this way, in each basic cell the occupational probability is the same for all atomic positions corresponding to a given tetrahedron.

At this stage of the process, 12 strong main reflections were found to be inconsistent with any tried model, showing high ΔF values, not caused by extinction. Several of them were axial $(h,0,0,0)$ reflections. As unit weights tend at most to reduce the differences between F_o and F_c, these reflections strongly conditioned the atomic x coordinates. This fact could be evidenced when a separate scale factor was allowed for these reflections. Nevertheless this artificial scale factor could not be justified when a check of the peak-profile quality was performed.

For this reason the refinements were repeated but using $1/\sigma^2(F)$ weighting and, therefore, reducing the importance of this set of reflections. With respect to the first weighting scheme, only small variations in R factors were found, although the goodness of fit increased to unusually large values (see Table 3). This fact indicates that standard deviations based on counting statistics are underestimated and/or the ratio between the number of observations and the number of parameters is near the lower limit in a

statistical sense. However, in spite of its questionable meaning, the decreasing goodness of fit in successive models suggests that the parallel reduction of R values could be significant. This point was checked by performing a Hamilton test (Hamilton, 1965) in which model IV was considered as unrestrained. In all cases this model was supported at a significance level higher than 99·5%.

Strictly speaking, this test cannot be applied directly to models which contain slack constraints (Pawley, 1972) but here the ratio between the number of observations and the number of slack constraints is high enough to disregard a more sophisticated model.

All refinements were carried out with a very small damping factor in order to avoid divergence. An analysis of the correlation matrix for the last model showed a complicated scheme of parameter interactions. It is remarkable for the strong correlations (both direct and through the amplitude of the displacement field along the a axis) between the x coordinates, the temperature-tensor elements β_{11} and the occupational probability amplitude for the atoms [Cu, Br(1) and Br(3)] lying near the $\{\sigma_x|\frac{1}{2},0,0,\frac{1}{2}\}$ plane.

Finally, a separate scale factor for satellites was refined, since a different behaviour for their intensities during the data collection could be expected as they had been measured after the main reflections (Zúñiga, Madariaga, Paciorek, Pérez-Mato, Ezpeleta & Etxebarria, 1989). Although the refinement showed a remarkable decrease in R factors for satellites, the values for both the second scale factor and the amplitudes of the displacive modulation (doubled for some atoms) were physically unreasonable. Probably, these meaningless values cover systematic errors caused either by uncorrected absorption or deviations in the internal scaling satellites.

Therefore in the next section we shall discuss model IV, which is considered to be the best one. In Table 3 the final R factors are listed together with the goodness of fit for each refined model. The average structure and the modulation parameters of model IV are presented in Tables 4, 5 and 6.* A projection along [001] of the average structure is shown in Fig. 1.

Discussion

As can be seen in Table 5, the rather high values of the occupational probability amplitudes indicate a

* Lists of structure factors and anisotropic atomic displacement parameters have been deposited with the British Library Document Supply Centre as Supplementary Publication No. SUP 53129 (8 pp.). Copies may be obtained through The Technical Editor, International Union of Crystallography, 5 Abbey Square, Chester CH1 2HU, England.

Table 4. *Average coordinates and equivalent atomic displacement parameters* ($Å^2 \times 10^2$) *of the incommensurate phase of* $[N(CH_3)_4]_2CuBr_4$

Estimated standard deviations of the last significant digits are given in parentheses. $U_{eq} = \frac{1}{3}\sum_i\sum_j U_{ij}a_i^*a_j^*\mathbf{a}_i.\mathbf{a}_j$.

	x	y	z	U (or U_{eq})
Cu	0·2559 (8)	0·4060 (2)	0·2377 (3)	6·2 (1)
Br(1)	0·2682 (9)	0·3755 (3)	0·0540 (3)	8·8 (1)
Br(2)	0·0190 (6)	0·3616 (5)	0·2804 (5)	11·8 (2)
Br(3)	0·2719 (9)	0·5409 (2)	0·3216 (3)	10·0 (2)
Br(4)	0·4690 (6)	0·3419 (4)	0·2976 (5)	10·0 (2)
N(1)	0·237 (4)	0·098 (1)	0·135 (1)	6·4 (5)
C(11)	0·291 (4)	0·112 (2)	0·243 (2)	9 (1)
C(12)	0·115 (4)	0·149 (2)	0·109 (3)	8 (2)
C(13)	0·217 (4)	0·008 (1)	0·122 (3)	8 (1)
C(14)	0·357 (4)	0·119 (2)	0·061 (3)	7 (1)
N(2)	0·249 (5)	0·667 (1)	0·005 (1)	6·3 (5)
C(21)	0·279 (4)	0·743 (1)	−0·062 (2)	6·5 (9)
C(22)	0·147 (3)	0·671 (2)	0·089 (3)	6 (1)
C(23)	0·214 (4)	0·595 (1)	−0·063 (2)	7 (1)
C(24)	0·390 (4)	0·645 (2)	0·051 (3)	9 (1)

Table 5. *Moduli* ($\times 10^4$) *and phases* ($/2\pi$) *of the displacive modulation functions for each atom*

Estimated standard deviations of the last significant digits are given in parentheses.

	A_1	φ_1	A_3	φ_3	A_2	φ_2
Cu	145 (7)	0·371 (7)	42 (5)	0·91 (4)	89 (7)	−0·05 (2)
Br(1)	270 (9)	0·285 (5)	16 (7)	0·52 (9)	104 (6)	−0·02 (1)
Br(2)	127 (7)	0·404 (9)	66 (8)	0·78 (2)	162 (8)	0·875 (9)
Br(3)	160 (10)	0·44 (1)	72 (5)	−0·17 (2)	30 (13)	0·04 (4)
Br(4)	112 (8)	0·43 (1)	86 (6)	0·01 (1)	143 (8)	0·100 (9)
N(1)	35 (35)	0·2 (2)	51 (40)	−0·3 (1)	47 (46)	0·0 (2)
C(11)	285 (66)	0·62 (4)	203 (32)	0·32 (4)	120 (37)	0·00 (5)
C(12)	228 (49)	0·44 (3)	245 (30)	0·54 (3)	234 (48)	0·75 (3)
C(13)	443 (60)	0·05 (2)	83 (29)	0·70 (6)	323 (38)	0·35 (3)
C(14)	202 (48)	0·19 (4)	294 (29)	0·86 (2)	238 (40)	0·04 (3)
N(2)	65 (37)	0·07 (9)	72 (34)	−0·07 (9)	68 (47)	0·3 (1)
C(21)	55 (50)	−0·1 (2)	89 (25)	0·32 (6)	303 (32)	0·33 (3)
C(22)	346 (50)	0·10 (2)	321 (28)	0·94 (2)	214 (37)	0·16 (3)
C(23)	368 (65)	0·66 (3)	122 (28)	0·32 (4)	236 (36)	0·98 (3)
C(24)	172 (47)	0·12 (4)	195 (36)	0·76 (3)	236 (45)	0·62 (3)

Table 6. *Moduli* ($\times 10^3$) *and phases* ($/2\pi$) *of the occupational modulation functions for each tetrahedron*

Estimated standard deviations of the last significant digits are given in parentheses.

Tetrahedron	P	ψ
$CuBr_4$	397 (11)	0·392 (6)
$(NC_4)_1$	216 (42)	−0·047 (33)
$(NC_4)_2$	208 (48)	0·132 (27)

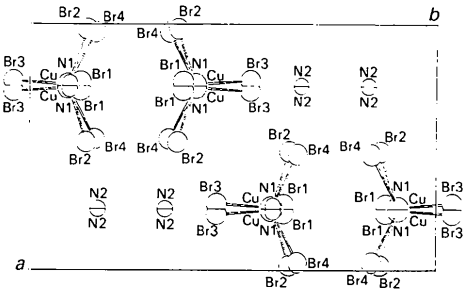

Fig. 1. Projection of the average structure of $[N(CH_3)_4]_2CuBr_4$ on to the ab plane. C atoms have been omitted for clarity.

progressive ordering from the basic structure to the lock-in phase. The amplitudes of the inorganic group are twice as large as those corresponding to the tetramethylammonium tetrahedra, which are equal within their standard deviations. This result suggests, as can be expected in this kind of compound, a higher degree of ordering for the inorganic groups. On the other hand (see Fig. 2) the occupational probability wave, corresponding to the organic tetrahedron labelled N_2C, is in antiphase (for this choice of the asymmetric unit) with the probability waves of the other two groups.

Interatomic distances and bond angles are listed in Tables 7 and 8. The distance variation in the incommensurate structure is (for distances involving the central atomic site and the corners of each tetrahedron), less than 0·1 Å. Of course this is, in part, a consequence of the refinement strategy. More important distance variations appear in C—C bonds (see Table 8) but in any case these are higher than 0·23 Å [C(11)—C(14) interatomic distance]. Table 8 also shows the Jahn–Teller distortion of the $CuBr_4$ tetrahedron.

Recently, Puget, Jannin, Perret, Godefroy & Godefroy (1989) have examined systematically the distortion of the inorganic tetrahedra within the A_2BX_4 family. The deformation has been characterized by means of two angles, θ and 2φ. For compounds with Cu ions, the mean values of θ and 2φ are 91·41 and 69·80° respectively. In the present case θ is the angle between the plane Br(2)Br(4)Br(1) and the plane Br(2)Br(4)Br(3), 2φ being the angle between the Br(1)Br(2) and Br(1)Br(4) lines. In the incommensurate phase both angles are periodic functions of the internal coordinate t, and their values oscillate (see Fig. 3) around an average value of θ = 90·33 and 2φ = 69·99°. This result reinforces in part the validity of the model since it could not be forced by the soft constraints of interatomic distances.

Table 7. *Interatomic distances* (Å) *in the incommensurate phase of* $[N(CH_3)_4]_2CuBr_4$

D_{min}, D_{max} and D_{av} are the minimum, maximum and average values of the modulated distances, respectively. Δ is the difference between the extremal distances. Estimated standard deviations of the last significant digits are given in parentheses.

	D_{min}	D_{max}	Δ	D_{av}
Cu—Br(1)	2·367 (4)	2·38 (1)	0·013	2·37 (1)
Cu—Br(2)	2·369 (9)	2·39 (1)	0·021	2·38 (1)
Cu—Br(3)	2·37 (1)	2·38 (1)	0·01	2·38 (1)
Cu—Br(4)	2·35 (1)	2·36 (1)	0·01	2·36 (1)
N(1)—C(11)	1·47 (2)	1·52 (6)	0·05	1·50 (6)
N(1)—C(12)	1·43 (3)	1·49 (6)	0·06	1·47 (6)
N(1)—C(13)	1·43 (2)	1·53 (6)	0·1	1·49 (6)
N(1)—C(14)	1·49 (6)	1·57 (6)	0·08	1·54 (6)
N(2)—C(21)	1·48 (6)	1·55 (5)	0·07	1·51 (6)
N(2)—C(22)	1·42 (3)	1·49 (6)	0·07	1·47 (6)
N(2)—C(23)	1·46 (2)	1·53 (6)	0·07	1·52 (6)
N(2)—C(24)	1·47 (6)	1·57 (6)	0·1	1·52 (6)

Table 8. *Bond angles* (°) *in the incommensurate phase of* $[N(CH_3)_4]_2CuBr_4$

α_{min}, α_{max} and α_{av} are the minimum, maximum and average values of the modulated bond angles, respectively. Δ is the difference between the extremal values. Estimated standard deviations of the last significant digits are given in parentheses.

	α_{min}	α_{max}	Δ	α_{av}
Br(1)—Cu—Br(2)	101·1 (6)	102·6 (6)	1·5	101·9 (6)
Br(1)—Cu—Br(3)	127·3 (8)	128·5 (9)	1·2	127·9 (8)
Br(1)—Cu—Br(4)	100·1 (6)	101·3 (6)	1·2	100·7 (6)
Br(2)—Cu—Br(3)	102·2 (6)	103·3 (6)	1·1	102·7 (6)
Br(2)—Cu—Br(4)	125·2 (6)	126·9 (7)	1·7	126·0 (6)
Br(3)—Cu—Br(4)	100·2 (6)	101·0 (5)	0·8	100·7 (6)
C(11)—N(1)—C(12)	107 (5)	118 (6)	11	112 (6)
C(11)—N(1)—C(13)	103 (5)	114 (6)	11	107 (5)
C(11)—N(1)—C(14)	104 (5)	111 (5)	7	108 (5)
C(12)—N(1)—C(13)	113 (5)	118 (6)	5	116 (6)
C(12)—N(1)—C(14)	103 (5)	118 (5)	15	110 (5)
C(13)—N(1)—C(14)	99 (5)	107 (5)	8	103 (5)
C(21)—N(2)—C(22)	118 (6)	124 (6)	6	121 (6)
C(21)—N(2)—C(23)	106 (5)	111 (5)	5	109 (5)
C(21)—N(2)—C(24)	100 (5)	107 (5)	7	103 (5)
C(22)—N(2)—C(23)	108 (5)	111 (5)	3	110 (5)
C(22)—N(2)—C(24)	105 (5)	111 (5)	6	108 (5)
C(23)—N(2)—C(24)	102 (5)	108 (5)	6	105 (5)

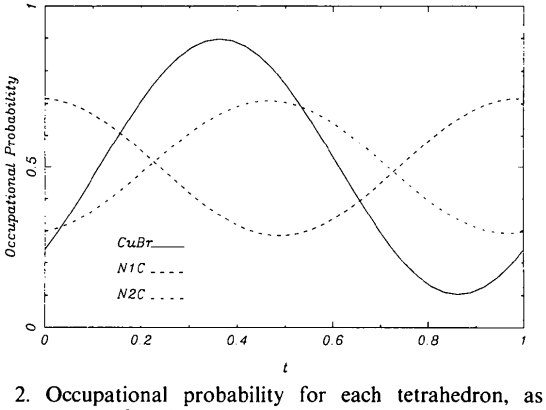

Fig. 2. Occupational probability for each tetrahedron, as a function of internal coordinate.

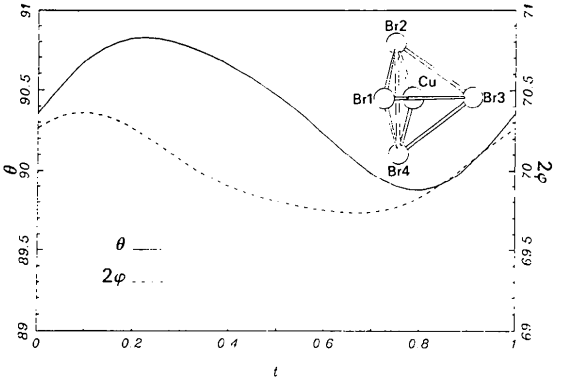

Fig. 3. Plot of θ and 2φ angles (°) along the internal coordinate. The tetrahedron indicates the labelling of the atoms used in the definition (see text) of such angles.

Table 9. *Amplitudes and phases (/2π) of the modulation functions corresponding to the fitted rigid-body model of the modulated structure of* $[N(CH_3)_4]_2CuBr_4$

The rotational (R) and translational (T) amplitudes are given in sexagesimal degrees and relative units. D is the agreement factor, described in the text.

Group	Direction	$R^{(0)}$	$T^{(0)}$	$R^{(1)}$	$\chi_{R^{(1)}}$	$T^{(1)}$	$\chi_{T^{(1)}}$
CuBr	x	0	0·0068	−2·387	−0·078	−0·0138	−0·132
	y	−3·169	0	−3·512	0·215	0·0043	−0·111
	z	−4·685	0	1·976	0·109	0·0089	−0·037
		$D^{(0)}=0·12$			$D^{(1)}=0·07$		
$(NC)_1$	x	0	−0·0067	16·751	−0·174	0·0020	0·0794
	y	15·897	0	−10·208	0·137	−0·0061	0·140
	z	−10·395	0	15·425	−0·007	0·0075	0·070
		$D^{(0)}=0·12$			$D^{(1)}=0·12$		
$(NC)_2$	x	0	0·0014	−16·364	−0·134	0·0051	0·040
	y	10·096	0	14·450	0·109	0·0064	−0·083
	z	−12·815	0	−9·940	0·090	−0·0048	−0·188
		$D^{(0)}=0·22$			$D^{(1)}=0·09$		

The small variations of interatomic distances and bond angles in the incommensurate structure, at least for the inorganic tetrahedron, permit the fitting of the incommensurate displacive distortion to rigid-body rotations and translations, which can be expressed in the form:

$$R_\alpha(t)=R_\alpha^{(0)}+R_\alpha^{(1)}\cos[2\pi(t+\chi_{R\alpha}^{(1)})] \quad (\alpha=x, y, z)$$

and similarly for rigid translations. The zeroth-order harmonic corresponds to movement from an ideal average structure, in which three atoms of each tetrahedra lie in the σ_x mirror plane, to the refined average positions. First-order harmonics have been calculated from atomic displacive amplitudes. Results of the fitting to rigid displacements are given in Table 9. The agreement between the observed atomic displacements (d_{obs}) and those obtained from the rigid-body model (d_{cal}) is measured by the index $D=[\sum(d_{cal}-d_{obs})^2/\sum d_{obs}^2]^{1/2}$. These agreement factors have rather good values even for the organic tetrahedra (with the exception of the homogeneous displacement in the N_2C group). Rotational and translational modulation functions are presented in Figs. 4 and 5. These show the antiphase relationships present in the rigid rotations corresponding to the organic tetrahedra, whereas the $CuBr_4$ rotations are in phase with one of the NC_4 groups. For rigid translations this type of phase relationship remains but the comparison is less clear.

A very good test of the reliability of the refined model consists of calculation of the lock-in distortion and a further comparison with the structure, if it is known. This is possible because for at least some of the A_2BX_4 compounds (Pérez-Mato, Gaztelua, Madariaga & Tello, 1986; Madariaga, Zúñiga, Pérez-Mato & Tello, 1987) the wavevector becomes commensurate at the lock-in transition point and the global phase of the modulation Φ is restricted to definite values, whereas the complex amplitudes of the modulation remain unchanged, excluding their normal temperature dependence.

On the other hand, the commensurate space groups corresponding to the superspace group $P(Pmcn)$:$(s\bar{1}1)$ have been derived for all possible values of Φ and $\mathbf{q}$ (Pérez-Mato, 1988). The space

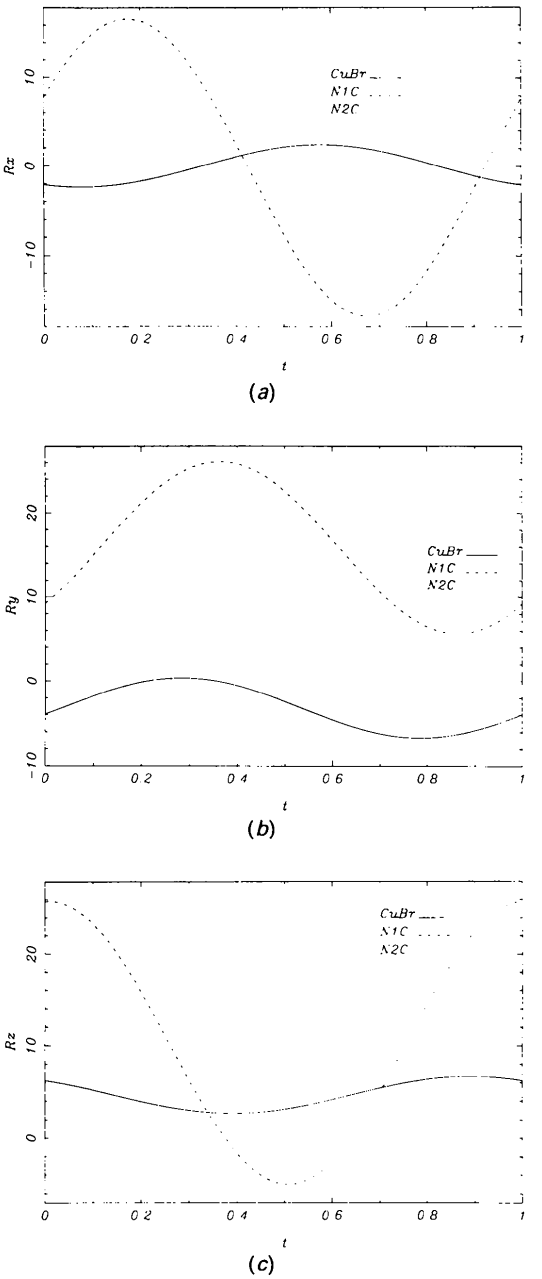

Fig. 4. Rotational modulation functions (*a*) R_x, (*b*) R_y and (*c*) R_z (°) *versus* the internal coordinate t.

groups deduced for a wavevector $\mathbf{q} = 0{\cdot}5\mathbf{b}^*$ can be summarized as follows:

$$P(Pmcn):(s\bar{1}1) \xrightarrow{\mathbf{q}=0{\cdot}5\mathbf{b}^*} \begin{cases} \Phi = \pm\pi/4 & Pbc2_1 \\ \Phi = 0 & P2_1/b11 \\ \Phi = \text{arbitrary value} & Pb11 \end{cases}$$

Therefore the lock-in distortion of $[N(CH_3)_4]_2CuBr_4$ will be characterized by a wavevector $\mathbf{q} = 0{\cdot}5\mathbf{b}^*$ and a global phase of $-\pi/4$ if the same origin as that used by Hasebe, Mashiyama & Tanisaki (1985) is desired. Using the incommensurate amplitudes (see Tables 5 and 6) and always choosing the configuration with the highest occupational probability, it is possible to extrapolate the lock-in distortion. Partial results for the central atom of each tetrahedron are given in Table 10(*a*).

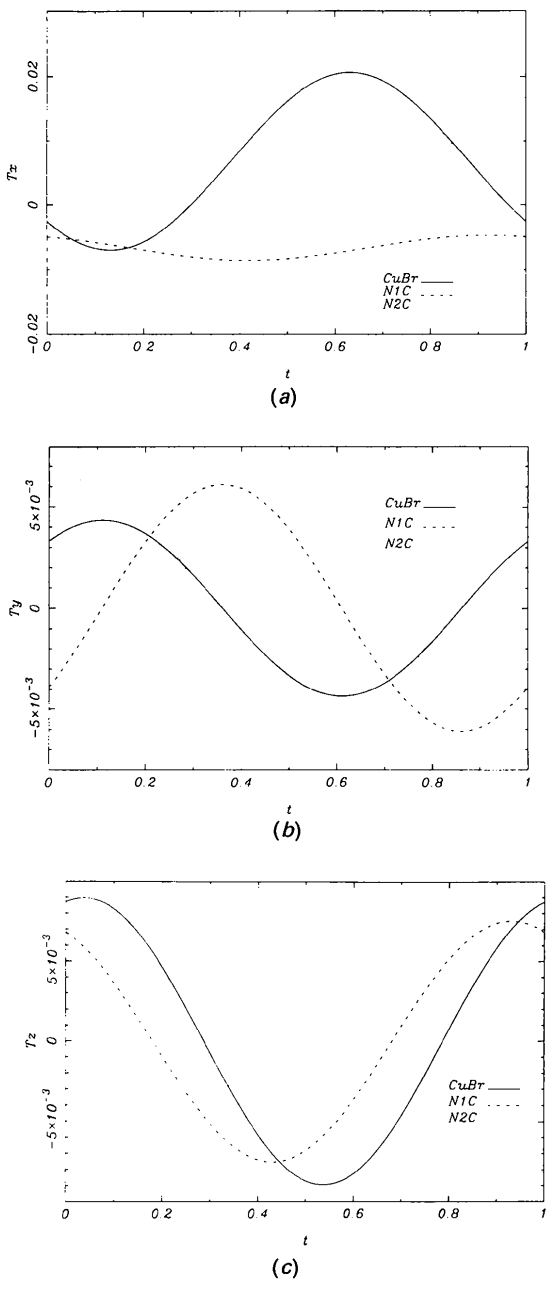

Fig. 5. Translational modulation functions (*a*) T_x, (*b*) T_y and (*c*) T_z in relative units, along the internal coordinate t.

Table 10. *Atomic coordinates of the central atom of each tetrahedron in the lock-in phase and in phase* II *of* $[P(CH_3)_4]_2CuBr_4$ *at* 293 K, *together with the corresponding coordinates extrapolated from the incommensurate distortion with the highest occupational probability*

The atom notation and number of significant digits were chosen according to the published structures.

(*a*) Lock-in structure

	Hasebe, Mashiyama & Tanisaki (1985)			Extrapolated structure		
	x	*y*	*z*	*x*	*y*	*z*
Cu(1)	0·2439	0·2011	0·2378	0·2395	0·2028	0·2395
Cu(2)	0·7297	0·2978	0·7692	0·7304	0·2991	0·7710
N(1)	0·244	0·050	0·135	0·234	0·050	0·138
N(2)	0·259	0·417	0·509	0·255	0·414	0·506
N(3)	0·755	0·452	0·863	0·739	0·453	0·862
N(4)	0·740	0·083	0·496	0·750	0·081	0·488

(*b*) $[P(CH_3)_4]_2CuBr_4$ structure

	Madariaga, Alberdi & Zúñiga (1990)			Extrapolated structure		
	x	*y*	*z*	*x*	*y*	*z*
Cu(1)	0·2156	0·19563	0·2208	0·2312	0·20140	0·2329
Cu(2)	0·7702	0·44474	0·2753	0·7624	0·45165	0·2697
P(1)	0·2442	0·2096	0·6162	0·2593	0·2035	0·6348
P(2)	0·2432	0·3264	0·0178	0·2460	0·3337	0·0104
P(3)	0·2476	0·0425	0·1201	0·2366	0·0483	0·1394
P(4)	0·2457	0·4237	0·5193	0·2525	0·4140	0·5009

Although the results are quite good, some discrepancies arise with respect to the peripheral atoms. However, direct atom-by-atom comparison with the lock-in structure (Hasebe, Mashiyama & Tanisaki, 1985) is not possible because the refined positions have not been constrained by any kind of penalty functions and the tetrahedra appear to be more distorted than in the present work. Nevertheless the result is further supported when the refined and the extrapolated structures are compared globally [see Figs. 6(*a*) and 6(*b*)].

Moreover, the same incommensurate distortion has been compared with the twofold (along **b**) structure of $[P(CH_3)_4]_2CuBr_4$ at 293 K (Madariaga, Alberdi & Zúñiga, 1990). Following the process indicated such distortion can be calculated with the same wavevector used for the lock-in phase extrapolation but putting $\Phi = 0$ as a global phase. Results of this calculation are given in Table 10(*b*) and graphic representations of both structures are given in Figs. 7(*a*) and 7(*b*). The results obtained confirm the validity of the proposed model and support the hypothesis of a continuous structural ordering throughout the incommensurate phase.

One of us (WAP) gratefully acknowledges the Spanish DGICYT for financial support. This work was supported by the Spanish DGICYT project No. PB87-0744.

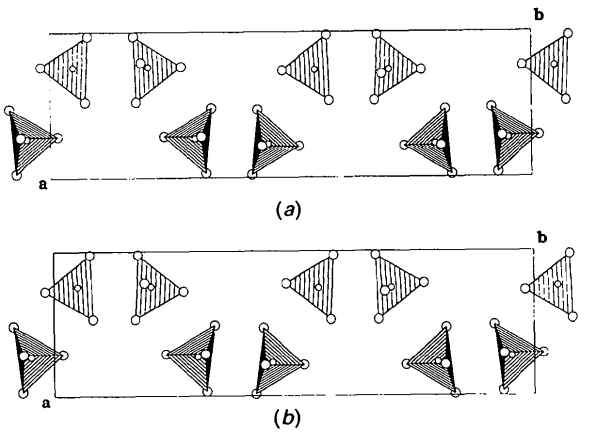

Fig. 6. Projection of the extrapolated (*a*) and refined (*b*) lock-in structures of $[N(CH_3)_4]_2CuBr_4$ onto the *ab* plane. Organic tetrahedra have been omitted for clarity. Cu and Br atoms are represented by small and large circles respectively.

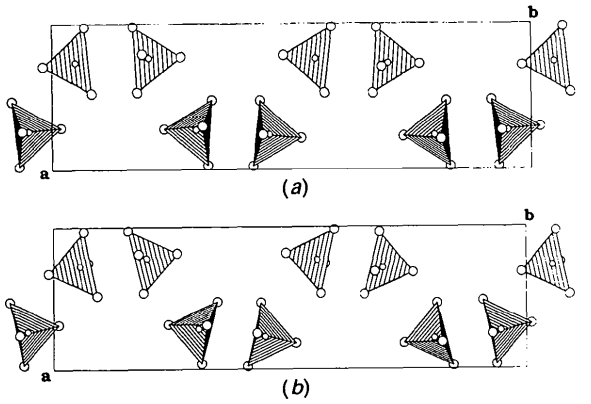

Fig. 7. Projection of the extrapolated (*a*) and refined (*b*) structures of $[P(CH_3)_4]_2CuBr_4$ onto the *ab* plane. Organic tetrahedra have been omitted for clarity. Cu and Br atoms are represented by small and large circles respectively.

References

ASAHI, T., HASEBE, K. & GESI, K. (1988). *J. Phys. Soc. Jpn*, **57**, 4219–4224.

CLAY, R., MURRAY-RUST, J. & MURRAY-RUST, P. (1975). *Acta Cryst.* B**31**, 289–290.

COSIER, J. & GLAZER, A. M. (1986). *J. Appl. Cryst.* **19**, 105–107.

FISCHER, R. X. (1985). *J. Appl. Cryst.* **18**, 258–262.

GESI, K. (1982). *J. Phys. Soc. Jpn*, **51**, 203–207.

GESI, K. (1983). *J. Phys. Soc. Jpn*, **52**, 2931–2935.

HAMILTON, W. C. (1965). *Acta Cryst.* **18**, 502–510.

HASEBE, K., MASHIYAMA, H. & TANISAKI, S. (1985). *Jpn. J. Appl. Phys.* **24**, 758–760.

International Tables for X-ray Crystallography (1974). Vol. IV, pp. 55, 99, 149. Birmingham: Kynoch Press. (Present distributor Kluwer Academic Publishers, Dordrecht.)

JANNER, A. & JANSSEN, T. (1980). *Acta Cryst.* A**36**, 399–415.

KELLER, E. (1989). *J. Appl. Cryst.* **18**, 258–262.

LÓPEZ-ECHARRI, A., RUIZ-LARREA, I. & TELLO, M. J. (1989). *Phys. Status Solidi B*, **154**, 143–152.

MADARIAGA, G., ALBERDI, M. M. & ZÚÑIGA, F. J. (1990). *Acta Cryst.* C**46**. In the press.

MADARIAGA, G., ZÚÑIGA, F. J., PÉREZ-MATO, J. M. & TELLO, M. J. (1987). *Acta Cryst.* B**43**, 356–368.

PACIOREK, W. A. & KUCHARCZYK, D. (1985). *Acta Cryst.* A**41**, 466–469.

PACIOREK, W. A., MADARIAGA, G. & ZÚÑIGA, F. J. (1990). *J. Appl. Cryst.* **23**. Submitted.

PACIOREK, W. A. & USZYNSKI, I. (1987). *J. Appl. Cryst.* **20**, 57–59.

PAWLEY, G. S. (1972). *Advances in Structure Research by Diffraction Methods*, Vol. 4, pp. 1–64. Oxford: Pergamon Press.

PÉREZ-MATO, J. M. (1988). *Solid State Commun.* **67**, 1145–1150.

PÉREZ-MATO, J. M., GAZTELUA, F., MADARIAGA, G. & TELLO, M. J. (1986). *J. Phys. C*, **19**, 1923–1935.

PÉREZ-MATO, J. M., MADARIAGA, G., ZÚÑIGA, F. J. & GARCÍA-ARRIBAS, A. (1987). *Acta Cryst.* A**43**, 216–226.

PUGET, R., JANNIN, M., PERRET, R., GODEFROY, L. & GODEFROY, G. (1989). Proc. 7th Int. Meet. Ferroelectr., 28 August–1 September 1989, Saarbrücken, Federal Republic of Germany.

STEWART, J. M., KRUGER, G. J., AMMON, H. L., DICKINSON, C. & HALL, S. R. (1972). The *XRAY* system – version of June 1972. Tech. Rep. TR-192. Computer Science Center, Univ. of Maryland, College Park, Maryland, USA.

TROUELAN, P., LEFEBVRE, J. & DEROLLEZ, P. (1984). *Acta Cryst.* C**40**, 386–389.

WOLFF, P. M. DE, JANSSEN, T. & JANNER, A. (1981). *Acta Cryst.* A**37**, 625–636.

YAMAMOTO, A. (1982). *Acta Cryst.* A**38**, 87–92.

ZÚÑIGA, F. J., MADARIAGA, G., PACIOREK, W. A., PÉREZ-MATO, J. M., EZPELETA, J. M. & ETXEBARRIA, I. (1989). *Acta Cryst.* B**45**, 566–576.